Development ePress. Posted online 16 October 2013
 | Development (2013) 140, 1-? doi:10.1242/dev.096024

RESEARCH ARTICLE

Knockdown of *col22a1* gene in zebrafish induces a muscular dystrophy by disruption of the myotendinous junction

Benjamin Charvet[1,*], Alexandre Guiraud[1,*], Marilyne Malbouyres[1], Daniela Zwolanek[2], Emilie Guillon[1], Sandrine Bretaud[1], Catherine Monnot[3], Jörg Schulze[2], Hannah L. Bader[1], Bruno Allard[4], Manuel Koch[2,5] and Florence Ruggiero[1,‡]

ABSTRACT

The myotendinous junction (MTJ) is the major site of force transfer in skeletal muscle, and defects in its structure correlate with a subset of muscular dystrophies. *Col22a1* encodes the MTJ component collagen XXII, the function of which remains unknown. Here, we have cloned and characterized the zebrafish *col22a1* gene and conducted morpholino-based loss-of-function studies in developing embryos. We showed that *col22a1* transcripts localize at muscle ends when the MTJ forms and that COLXXII protein integrates the junctional extracellular matrix. Knockdown of COLXXII expression resulted in muscular dystrophy-like phenotype, including swimming impairment, curvature of embryo trunk/tail, strong reduction of twitch-contraction amplitude and contraction-induced muscle fiber detachment, and provoked significant activation of the survival factor Akt. Electron microscopy and immunofluorescence studies revealed that absence of COLXXII caused a strong reduction of MTJ folds and defects in myoseptal structure. These defects resulted in reduced contractile force and susceptibility of junctional extracellular matrix to rupture when subjected to repeated mechanical stress. Co-injection of sub-phenotypic doses of morpholinos against *col22a1* and genes of the major muscle linkage systems showed a synergistic gene interaction between *col22a1* and *itga7* (α7β1 integrin) that was not observed with *dag1* (dystroglycan). Finally, pertinent to a conserved role in humans, the dystrophic phenotype was rescued by microinjection of recombinant human COLXXII. Our findings indicate that COLXXII contributes to the stabilization of myotendinous junctions and strengthens skeletal muscle attachments during contractile activity.

KEY WORDS: Collagen, Extracellular matrix, Muscular dystrophy, Myotendinous junction, Skeletal muscle, Zebrafish

INTRODUCTION

The myotendinous junction (MTJ) represents the major site of muscle force transmission to tendons. This highly specialized structure displays finger-like folds that increase contact between muscle and tendon. Complex and dynamic interactions between muscle sarcolemma and extracellular matrix (ECM) components occur at the MTJ, and form trans-sarcolemmal linkage systems that are required for the initiation and maintenance of muscle fiber attachment to tendon. These interactions provide a continuous structural link between intracellular cytoskeleton, sarcolemma and ECM proteins, such as the basement membrane (BM) component laminin. Two independent trans-sarcolemmal linkage systems are present at MTJs: the dystrophin-glycoprotein complex (DGC) and the α7β1 integrin complex. Whereas α7β1 integrin binds only to laminin and was reported to localize primarily at the MTJ, α-dystroglycan interacts with several BM components and distributes along the sarcolemma (Han et al., 2009). DGC and α7β1 integrin are both crucial for maintaining skeletal muscle integrity and attachments, but a functional overlap between the two linkage systems remains undemonstrated (Rooney et al., 2006; Han et al., 2009).

Mutations in most of the genes encoding components of the linkage complexes result in muscle disorders (Carmignac and Durbeej, 2012). In humans, mutations in the dystrophin gene cause Duchenne and Becker muscular dystrophies, whereas mutations in sarcoglycan genes are responsible for some forms of limb girdle muscular dystrophies (Cohn and Campbell, 2000). Mutations in the integrin α7 gene (*ITGA7*) cause congenital myopathy (Hayashi et al., 1998) and the most common form of congenital muscular dystrophy MDC1A is associated with loss of functional laminin α2 (Helbling-Leclerc et al., 1995). The impact of these mutations in MTJ formation and/or function is still poorly documented, particularly in the context of human diseases. However, mice that lack dystrophin (*mdx*; *Dmd* – Mouse Genome Informatics) (Law and Tidball, 1993; Law et al., 1995), laminin α2 (*dy*; *Lama2* – Mouse Genome Informatics) (Desaki, 1992) or integrin α7 (Miosge et al., 1999; Welser et al., 2009) exhibit a striking reduction in the number of membrane folds at MTJ that impairs its function and results in progressive muscular dystrophy.

Collagen XXII (COLXXII) is a distinctive BM component for it is strictly localized at tissue junctions, specifically at the MTJ (Koch et al., 2004). It belongs to the FACIT (fibril-associated collagens with interrupted triple helix) subset of the collagen superfamily, the members of which are known to associate with collagen fibers through their C-terminal collagenous domains and to mediate protein-protein interactions through their N-terminal non-collagenous domains (Ricard-Blum and Ruggiero, 2005). The function of COLXXII remains unknown, but its enrichment at the MTJ, as well as the high capacity of FACIT members to associate with other matrix components suggests that COLXXII may contribute to the mechanical stability of the MTJ.

Zebrafish is becoming instrumental for specifically addressing the extent to which the loss of MTJ components contributes to muscle physiology and pathology (Ingham, 2009). In zebrafish, somitic muscle fibers differentiate to span the entire myotome and

[1]Institut de Génomique Fonctionnelle de Lyon, ENS de Lyon, UMR CNRS 5242, Université Lyon 1, 46 Allée d'Italie, 69364 Lyon cedex 07, France. [2]Center for Biochemistry, Medical Faculty, University of Cologne, D-50931 Cologne, Germany. [3]Centre Interdisciplinaire de Recherche en Biologie, CNRS UMR 7241/INSERM U1050, Collège de France, Paris, France. [4]Centre de Génétique et de Physiologie Moléculaire et Cellulaire, Université de Lyon, Université Lyon 1, CNRS UMR 5534, 69622 Villeurbanne Cedex, France. [5]Institute for Dental Research and Oral Musculoskeletal Biology, Center for Molecular Medicine Cologne, Medical Faculty, University of Cologne, D-50931 Cologne, Germany.
*These authors contributed equally to this work

‡Author for correspondence (florence.ruggiero@ens-lyon.fr)

Received 17 March 2013; Accepted 27 August 2013

Development (2013) doi:10.1242/dev.096024

vertical myosepta, which are functionally equivalent to the mammalian tendon and serve as attachment sites at myotome borders where the MTJ forms (Henry et al., 2005; Charvet et al., 2011). Zebrafish dystrophic mutants and morphants with skeletal muscle abnormalities represent informative models of muscle disease pathogenesis (Ingham, 2009; Sztal et al., 2012) and therapy, as reported recently (Kawahara et al., 2011). The detachment of muscle fiber at the MTJ is a common phenotypic feature of several dystrophic mutants and/or morphants, e.g. *sapje*/dystrophin (*sap*) (Bassett et al., 2003; Guyon et al., 2009), *candyfloss*/laminin α2 (*caf*) (Hall et al., 2007) and *patchytail*/dystroglycan (Gupta et al., 2011), and the integrin α7 morphants (Postel et al., 2008). The integrin-linked kinase (ILK)-deficient *loss-contact* (*loc*) (Postel et al., 2008) and laminin-β2-deficient *softy* (*sof*) (Jacoby et al., 2009) mutants also exhibit destabilization of muscle attachments at intracellular (*loc*) and extracellular (*sof*) sides of the MTJ, suggesting that these genes are also important for maintenance of muscle attachments. In most of these mutants, skeletal muscles develop normally but the onset of muscle contractions provokes progressive muscle cell detachment from their insertion site and the subsequent degeneration of the axial myotome (Sztal et al., 2012).

In the present study, we have cloned and characterized the zebrafish ortholog of the human *COL22A1* gene, *col22a1*, and showed that the protein product COLXXII is specifically expressed by skeletal muscle and deposited at the junctional ECM as the MTJ develops. We show that *col22a1* knockdown in zebrafish embryos resulted in muscle dysfunction indicative of dystrophic phenotype. Synergistic interactions suggest that COLXXII contributes to the stabilization of the integrin α7β1 linkage system. Pertinent to a conserved role in humans, the dystrophic phenotype was rescued by microinjection of human COLXXII. Our findings provide functional evidence for a role of *col22a1* in the stabilization and maintenance of the MTJ.

RESULTS

Zebrafish *col22a1* presents the overall structure of its mammalian counterparts

A zebrafish ortholog of the human *COL22A1* gene is available in the CoreNucleotide database (http://www.ncbi.nlm.nih.gov). The prediction of the zebrafish COLXXII α1 chain mRNA (XM_685915.3 version GI:189532156) was incomplete but corresponds well to the human and mouse COLXXII α1 chain. We thus decided to clone and sequence the complete zebrafish *col22a1* cDNA. To this aim, we subjected the predicted zebrafish COLXXII α1 chain mRNA sequence to a blastn (http://blast.ncbi.nlm.nih.gov/Blast.cgi) against *Danio rerio* genomic sequences. This blast retrieved the *Danio rerio* strain Tuebingen unplaced genomic scaffold, Zv9_NA466 (NW_003336732.1). Using this sequence, we designed primers to obtain the complete sequence through PCR amplification of 24 hpf embryo cDNA. The sequence (accession number HE_981211; 4925 bp) included full coding sequence (4869 bp) and a part of the 5′ and 3′ UTR sequences. The protein deduced from the coding sequence contains 1622 amino acids (protein id CCK86746.1).

Alignments of the zebrafish COLXXII α1 chain with the human, mouse and chicken orthologs revealed an overall 60% identity and about 70% similarity (supplementary material Fig. S1; Table 1). The overall structure is similar to that of other vertebrates and contains the structural signatures of all FACITs (Ricard-Blum and Ruggiero, 2005) (supplementary material Fig. S1). The only difference from the human COLXXII, but shared with mouse and chicken orthologs, was the absence of the NC4 linker sequence (supplementary material Fig. S1). As such, a transcript without NC4 was the unique transcript detected in developing zebrafish (supplementary material Fig. S2).

Table 1. Comparison between the collagen XXII α1 chain zebrafish (HE_981211) and human (NP_690848.1), mouse (NP_081450.1) and chicken (NP_001132911.1) orthologs

Species	Domains	Identity (%)	Similarity (%)
Homo sapiens	Full length	59	71
	VWA	70	85
	TSPN	67	85
Mus musculus	Full length	59	72
	VWA	69	87
	TSPN	68	87
Gallus gallus	Full length	60	74
	VWA	73	89
	TSPN	69	86

Numbers represent the percentage of identity and similarity obtained from alignments using ClustalW. TSPN, thrombosponin N-terminal-like domain, VWA, von Willebrand factor A-like domain.

col22a1 is expressed in skeletal muscle and its protein product localizes at the MTJ

The expression pattern of zebrafish *col22a1* was analyzed at the transcriptional level by RT-PCR (Fig. 1A) and whole-mount *in situ* hybridization (Fig. 1B). By RT-PCR, we first detected *col22a1* expression at 22 hpf, during the third stage of segment boundary formation, as defined by Henry et al. (Henry et al., 2005). At 24 hpf, transcript level increased and expression was then maintained in developing embryos (Fig. 1A). *In situ* hybridization of 24 hpf embryos revealed a diffuse signal within the somites with no signal at myotome boundaries (Fig. 1B,a). As embryos developed, expression concentrated to muscle cell extremities close to vertical myosepta (Fig. 1B,b-e).

Protein expression in developing embryos was then assessed by western blot of whole-protein extracts using our specific polyclonal antibodies raised against a zebrafish COLXXII recombinant domain (supplementary material Fig. S3A,B). Two bands were detected from 24 hpf: one migrating at 200 kDa corresponding to the expected molecular weight of COLXXII α1 chain and an upper band that likely corresponds to partial non-reducible dimers (Fig. 1C), as reported for the mammalian COLXXII (Koch et al., 2004). Using confocal microscopy, COLXXII was detected in 26 hpf myotomes as a fuzzy signal, which became more intense along the myosepta (Fig. 1D,a). As embryo developed, COLXXII became restricted to myotomes boundaries (Fig. 1D,b,c). In addition, as revealed by whole-mount double immunostaining of 72 hpf embryos (Fig. 1D,c-e), COLXXII colocalized at the confocal resolution with the membrane-associated dystrophin that is enriched at junctional sarcolemma in zebrafish. Moreover, at later larval stage (5 dpf), when MTJ is fully differentiated and forms deep sarcolemmal folds (Charvet et al., 2011), COLXXII antibodies specifically decorated MTJ interdigitations (supplementary material Fig. S3E). Finally, COLXXII was detected in adult MTJs, suggesting a role for COLXXII throughout life (supplementary material Fig. S3C,D). *Col22a1* transcript was also detected in the head and the pectoral fins of 48 hpf (not shown) and 72 hpf (Fig. 1B,d) embryos, but signal was barely visible at the protein level (Fig. 1D,b). Collectively, our data identify *col22a1* as a specific marker of developing and mature zebrafish MTJs.

Development (2013) doi:10.1242/dev.096024

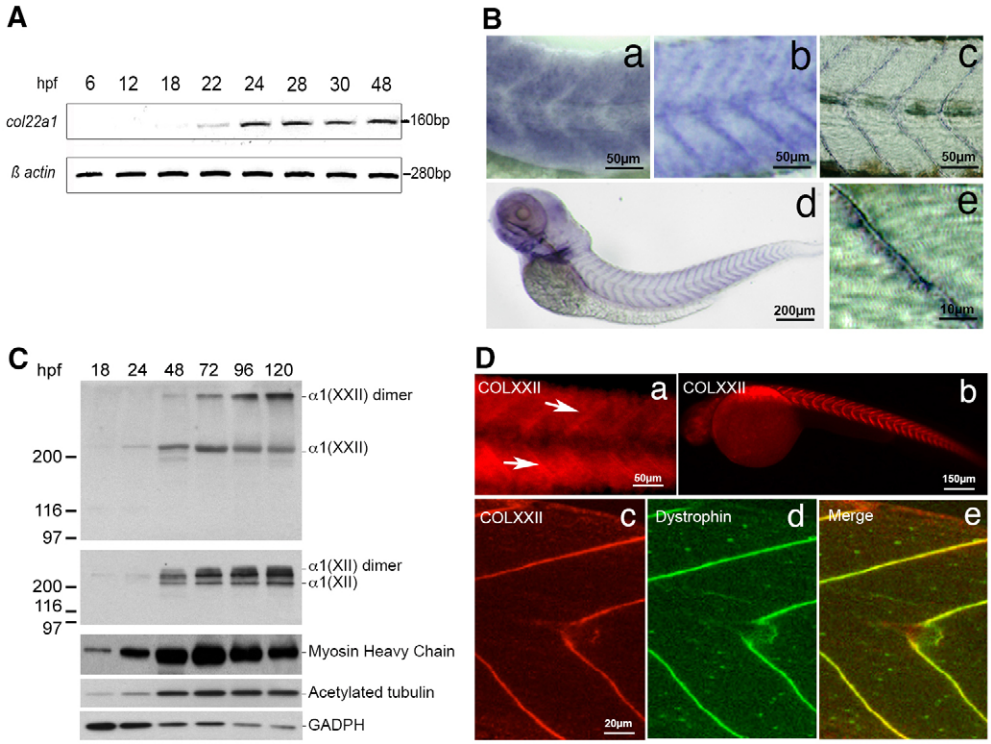

Fig. 1. Expression and distribution of zebrafish *col22a1* mRNA and protein. (A) RT-PCR analysis of zebrafish *col22a1* at different developmental stages. β-Actin was used as a loading control. (B) Whole-mount *in situ* hybridization with *col22a1* antisense probe in the trunk of 24 hpf (a), 48 hpf (b) and 72 hpf (c) embryos. Lateral view of a 72 hpf whole embryo (d) and zoomed image of a somite boundary (e). (a-e) Lateral views with anterior to the left; (a-c) somites in the posterior region of yolk extension are shown. Scale bars: 50 µm in a-c; 200 µm in d; 10 µm in e. (C) Western blot with anti-COLXXII of protein extracts from animals at different stages. COLXII and myosin heavy chain antibodies were used as collagen and late muscle differentiation marker controls, respectively. Antibodies to GAPDH and acetylated tubulin were used as loading controls. Number on the left indicate sizes (in kDa) of protein standard markers. hpf, hour post-fertilization. (D) Lateral views of whole-mount immunofluorescence staining with anti-COLXXII of 26 hpf (a) and 48 hpf (b) embryos. (a) Arrows indicate COLXXII staining that concentrated along myosepta. (c-e) Double immunostaining of a 72 hpf embryo with anti-COLXXII (c, red), dystrophin (d, green) and merge (e). Anterior is towards the left. Scale bars: 50 µm in a; 150 µm in b; 20 µm in c-e.

col22a1 knockdown leads to a muscular dystrophy-like phenotype

To elucidate the function of COLXXII, morpholino-mediated knockdown was performed in zebrafish. The specificity and efficiency of the morpholinos targeting *col22a1* (MO22a and MO22b) was evidenced by western blotting (Fig. 2A) and immunofluorescence staining (Fig. 2B). We also examined the expression levels of collagen XII (COLXII), which is a FACIT collagen expressed in myosepta (Bader et al., 2009), in MO22-injected and uninjected embryos. We showed that COLXII protein levels (Fig. 2C) and *col12a1a* gene expression (supplementary material Fig. S4A) did not change significantly, which is indicative of a specific effect of MO22 on the target gene. Injection of MO22a or MO22b in one- to two-cell embryos resulted in normal embryos during the first day of development. At 48 hpf, MO22a- and MO22b-injected embryos exhibited identical gross phenotype characterized by a slight (moderate phenotype) or pronounced (severe phenotype) curvature of the tail and trunk (Fig. 2C; supplementary material Table S2 for percentages of embryos in each class). The extent of inhibition of COLXXII protein expression correlated with the severity of the phenotype (supplementary material Fig. S5). The curvature phenotype became progressively more severe with time, which is indicative of the progressive nature of the phenotype (Fig. 2C, histogram). Higher magnification views of the trunk region of 96 hpf larvae revealed that, independently of phenotype severity, somites displayed abnormal U-shape morphology, which is indicative of muscle defects (Fig. 2D). Muscle defects can correspond to defective muscle differentiation. COLXXII protein was detected from 24 hpf, a time when muscle differentiation is completed (Blagden et al., 1997). In support of this, the time-course expression of the late myogenic marker MHC was similar in MO22-injected and uninjected embryos, suggesting that muscles have differentiated normally (Fig. 2B). In addition to morphological defects, MO22-injected embryos generally failed to hatch and chorions have to be removed manually. Finally, unlike uninjected larvae (supplementary material Movie 1), MO22-injected larvae displayed swim failure and motility impairment after touch stimulation (supplementary material Movie 2). As the two sequence-independent morpholinos against *col22a1* (MO22a and MO22b) yielded identical results, we used them indifferently in all the following experiments and they will be referred as to MO22 hereafter.

The level of birefringence of the trunk muscle under polarized light is commonly used to quantify the level of muscle damage in zebrafish (Sztal et al., 2012). We thus quantified the level of birefringence in 4 dpf MO22-injected larvae with moderate phenotype and compared with larvae of the same age injected with morpholinos against *lama2* (MO-*lama2*) and *itga7* (MO-*itga7*), which have been reported to cause a dystrophic muscle phenotype (Hall et al., 2007; Postel et al., 2008). The percentage of birefringence was significantly reduced in larvae injected with MO22 (n=10; P<0.001) as for larvae injected either with MO-*lama2* (n=10; P<0.05) or MO-*itga7* (n=10; P<0.001) (Fig. 2E). Although reduction of birefringence in *col22a1* morphants was similar to that

Development (2013) doi:10.1242/dev.096024

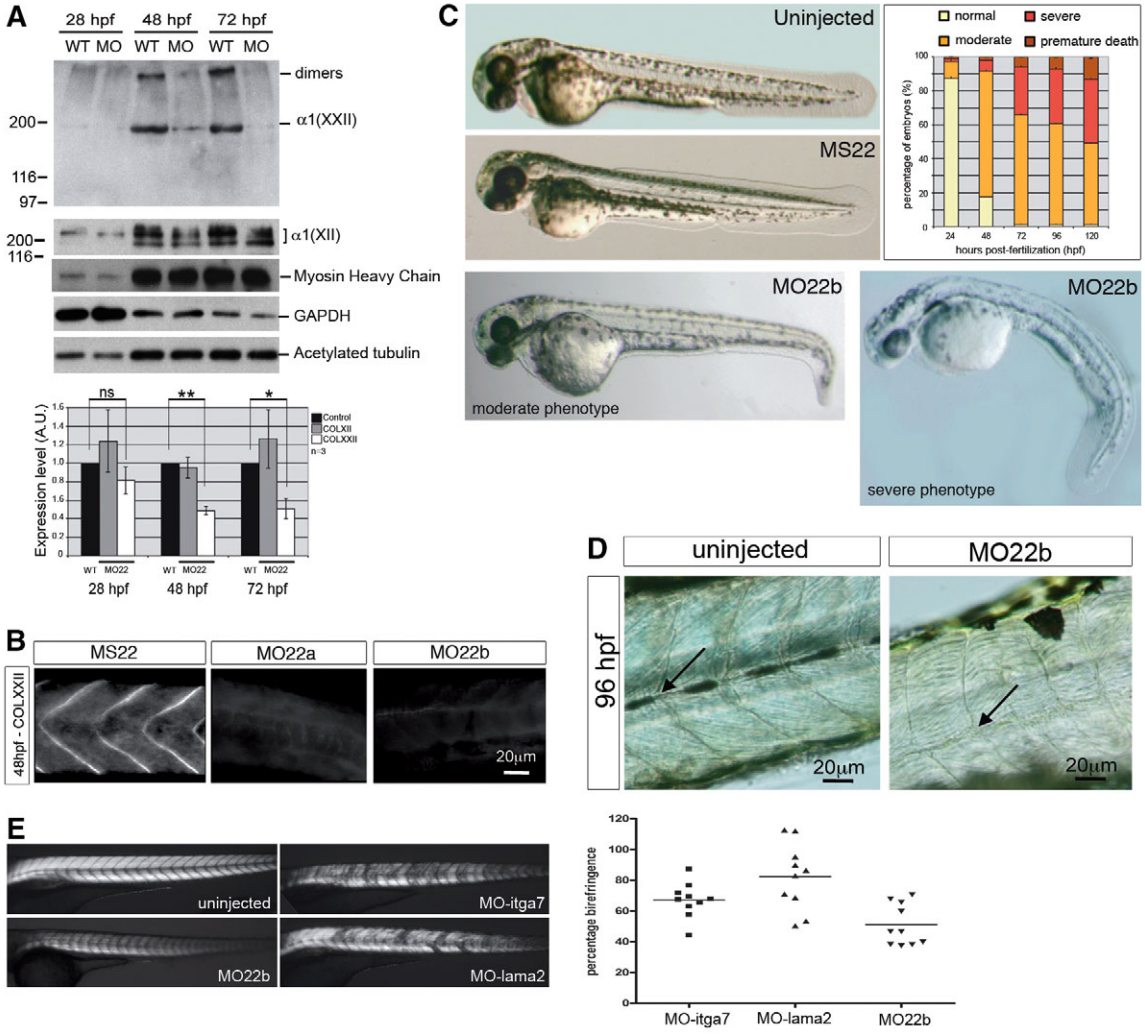

Fig. 2. Morpholino knockdown of *col22a1* in developing zebrafish. (A,B) Efficacy, specificity and functional duration of *col22a1* morpholino-knockdown in developing embryos. (A) Western blots of MO22b-injected (MO) and uninjected (WT) embryo protein extracts with antibodies to COLXXII, myoseptal marker COLXII or myosin heavy chain. Loading controls are GAPDH and acetylated tubulin. Data from one representative experiment are shown. Histogram shows densitometric quantification of relative COLXXII and COLXII expression levels normalized to acetylated tubulin. Data are mean±s.e.m. (n=3), *P<0.05, **P<0.01. (B) Immunofluorescence with antibodies to COLXXII of 48 hpf embryos injected with MO22a, MO22b and five-base mismatch morpholino (MS22). Scale bars: 20 μm. (C,D) Light microscopy analysis of the phenotype. (C) Representative images of 48 hpf uninjected embryos, embryos injected with control MS22, and moderate and severe phenotypes of *col22a1* morphants (MO22b). Histogram shows percentage of MO22-injected larvae displaying no, moderate or severe phenotypes at different developmental stages (n=250; number of injections=3). (D) U-shaped somites of 96 hpf MO-injected larvae (MO22b) compared with the V-shape somites of uninjected larvae (arrows). Scale bars: 20 μm. (E) Birefringence of 4 dpf MO22-injected larvae. Representative images of larvae injected with morpholinos against *col22a1* (MO22, moderate phenotype), *lama2* (MO-lama2) and *itga7* (MO-itga7) compared with uninjected larvae. Quantification of birefringence measurements. Values represent mean birefringence normalized to uninjected larvae. Anterior is towards the left.

obtained with the *itga7* and *lama2* dystrophic morphants (Fig. 2E, histogram), *col22a1* morphants did not exhibit a stochastic muscle detachment phenotype, as observed in MO-*lama2* or MO-*itga7* larvae (Fig. 2E, left panel). The reduction of birefringence in MO22-injected larvae was rather caused by a general disorganization of muscles, including larger dark zones at myotome boundaries. When combined, our results showed that loss of COLXXII leads to defects that are indicative of a muscular dystrophic-like phenotype.

col22a1 knockdown causes muscle weakness and contraction-induced fiber detachment

The impaired swimming activity of *col22a1* zebrafish suggested defects in muscle force generation. We thus investigated the repercussions of *col22a1* knockdown on electrically evoked skeletal muscle contractile performance at 5 dpf. Repeated twitch contractions elicited in uninjected larvae exhibited stable amplitudes (Fig. 3A). In MO22-injected larvae, the contractile force was considerably decreased and the mean amplitude of the twitch response was about eight times smaller. Given the localization of COLXXII, this muscle weakness likely resulted from reduced force transmission, although a decrease in the number of functional fibers involved in force development cannot be excluded. We indeed occasionally observed muscle detachment in morphants (Fig. 3B). Acridine Orange exclusively stained the retracted fibers, indicating that muscle fibers underwent cell death only after they detach (Fig. 3B). Histology analysis of 5 dpf MO22-injected larvae revealed cell-free spaces in myotomes (Fig. 3B), resulting from muscle fiber detachment and retraction. In addition, the myosepta

Development (2013) doi:10.1242/dev.096024

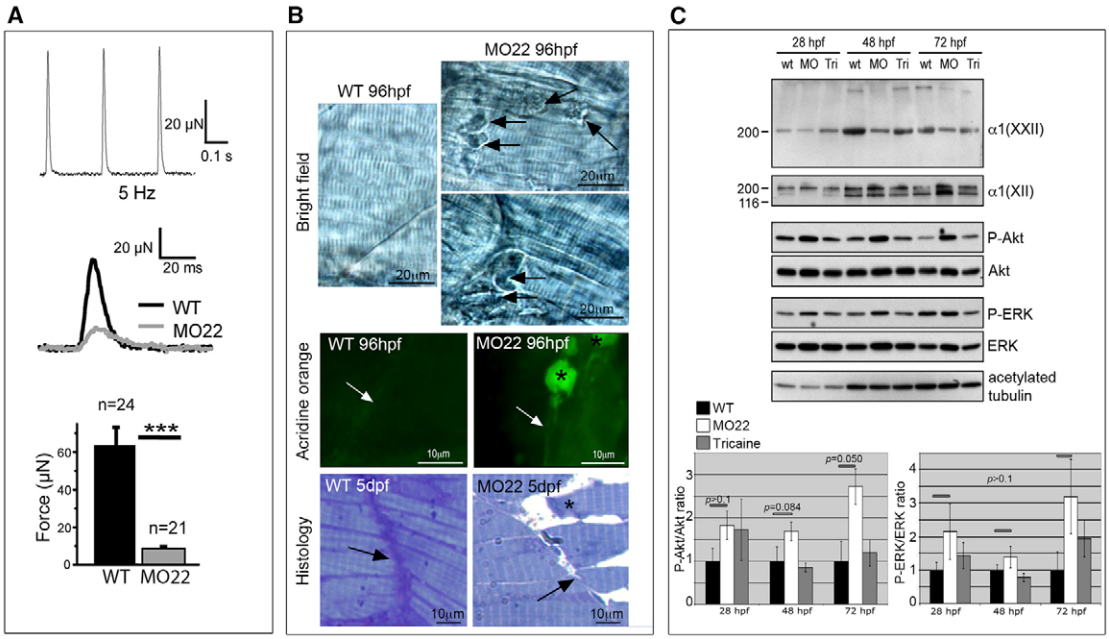

Fig. 3. *col22a1* knockdown leads to muscular dystrophic phenotype. (A) Recording of contraction in response to single supramaximal electric shocks applied to wild-type and MO-22-injected larvae. Twitch responses (middle panel) and mean contraction amplitudes (bottom panel) of 5 dpf wild-type (black) and MO22-injected (gray) larvae. Data are mean±s.e.m. ***P<0.001. (B) 96 hpf uninjected (WT) and MO22-injected (MO22) larvae. Light microscopy (top panel) revealed muscle detachment and retraction (MO22, arrows) from vertical myoseptum. Acridine Orange staining (middle panels): asterisks point to Acridine Orange-positive retracted muscle fibers in MO22 and arrows indicate myoseptum. Histology (bottom panels) of MO22 shows cell-free spaces, reduced MTJ interdigitations (arrows) and clear appearance of myosepta compared with WT. Asterisk indicates a detached and retracting muscle fiber. (C) Western blots with antibodies to phospho-Akt (P-Akt) and total Akt protein (Akt) or phospho-ERK1/2 (P-ERK1/2) and total ERK protein (ERK1/2) of extracts from uninjected (wt) and tricaine-treated (Tri) wild-type and MO22-injected (MO) embryos at different stages. Loading controls are antibodies to COLXII and acetylated tubulin. Data from one representative experiment are shown. Only one band is detected with ERK1/2 antibodies, as reported for zebrafish (Ng et al., 2012). Histograms show densitometric quantification. Phospho-protein levels were normalized against total protein levels. Data are mean±s.e.m. (n=3).

and MTJ displayed perturbed morphology. The myosepta appeared larger and exhibited a clear appearance and the MTJs had lost their interdigitations (Fig. 3B), two structural defects that may also cause muscle weakness. Collectively, these data indicate that COLXXII is crucial for force development, and the integrity and maintenance of muscle attachments.

col22a1 knockdown leads to increased phosphorylation of the survival factor Akt

An increase in the phosphorylation of the survival factors Akt (Peter and Crosbie, 2006; Kim et al., 2011) and ERK (Boppart et al., 2011) was reported in dystrophic skeletal muscles and interpreted as a compensatory mechanism that counteracts muscle waste. We therefore investigated the activation of Akt and ERK in skeletal muscles of decapitated and deyolked MO22-injected and wild-type embryos. Because mechanical forces have also been reported to induce Akt and ERK activation (Mohamed et al., 2010), in parallel with uninjected embryo controls, we raised wild-type embryos under anesthetizing (tricaine) conditions to inhibit muscle contractions. Contrary to controls, phosphorylation of Akt (P-Akt) significantly increased in MO22-injected embryos when substantial increase of embryo movement occurs within chorion (48 hpf) and at time of hatching (72 hpf) (Fig. 3C). We also detected similar elevation of the levels of ERK phosphorylation (P-ERK) though not significant (Fig. 3C). Unexpectedly, a decrease in COLXXII levels was observed in embryos treated with tricaine that was comparable with the reduction observed in 72 hpf MO22-injected embryos (Fig. 3C), suggesting that mechanical stress can regulate COLXXII. Hence, our data show that the reduction of COLXXII expression does not activate Akt when embryos are raised under anesthetic that suppresses contractile activity and the incidence of muscle injury. Instead, in unanesthetized embryos, knockdown of COLXXII expression caused contraction-induced muscle damage that resulted in a compensatory mechanism promoting cell survival through Akt activation. Similar results were obtained for p-ERK (Fig. 3C). In conclusion, contraction-induced injury is responsible for the activation of Akt in morphant skeletal muscles, most likely to compensate for muscle waste induced by COLXXII deficiency.

COLXXII is required for strengthening MTJ stability at the junctional extracellular matrix

To determine the origin of muscle weakness and to detail the site of rupture leading to muscle fiber detachment, we next examined, using transmission electron microscopy (TEM), the ultrastructure of skeletal muscle of morphants. In agreement with the above western blot data that showed normal MHC expression (Fig. 2A), we did not detect any changes in the ultrastructure of the contractile system and triadic structures of morphants (Fig. 4B) when compared with uninjected larvae (Fig. 4A). Thus, lack of COLXXII did not prevent muscle fiber formation and differentiation. Sarcolemma was tightly associated to the junctional BM in MO22-injected larvae (Fig. 4D). As in controls (Fig. 4C), the BM formed a continuous layer, although, in some areas, its thickness appeared irregular (Fig. 4D). Remarkably, and in support of our histology data (Fig. 3B), MTJs lacked almost completely sarcolemmal folding in MO22-injected larvae (compare Fig. 4D with control in 4C). In addition, morphant

Development (2013) doi:10.1242/dev.096024

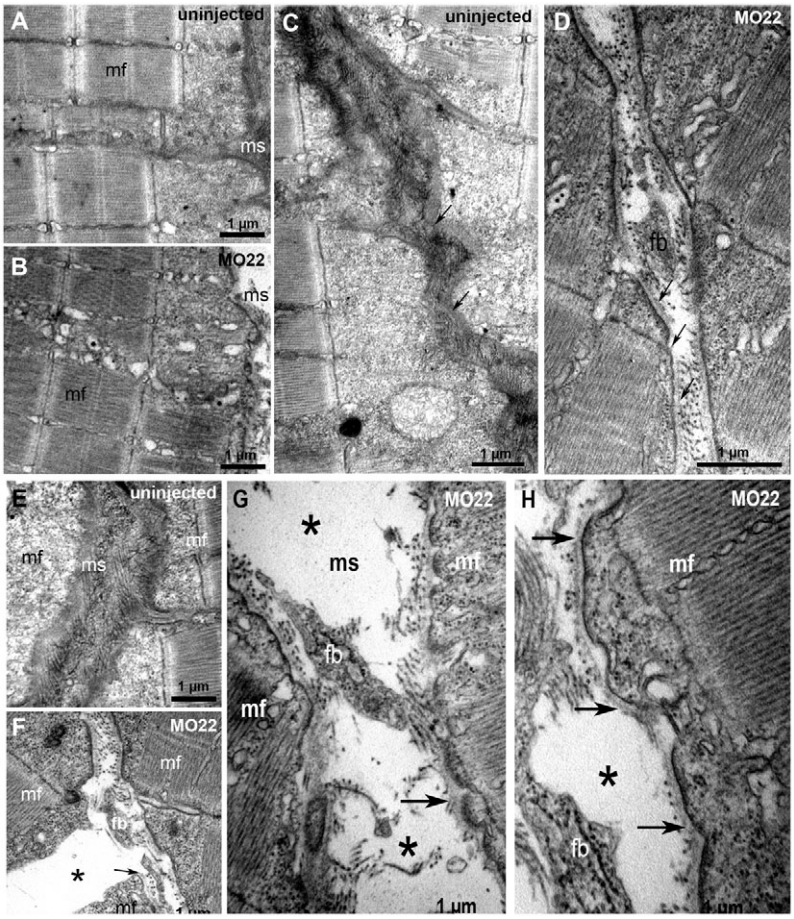

Fig. 4. TEM reveals defects in MTJ and myosepta ultrastructure, and identifies the rupture site at the outer surface of the basement membrane. Micrographs of 5 dpf uninjected (A,C,E) and MO22-injected (B,D,F-H) larvae. (A,B) Sarcomeric organization of skeletal muscle in morphants (B) and uninjected larvae (A). (C,D) Detail of the sarcolemma and basement membrane structure (arrows) in wild type (C) and morphants (D). (E-H) Detail of MTJ and myoseptum structure in wild type (E) and morphants (F-H). Asterisks show a gap corresponding to detached and retracted fiber (F) and tears between myoseptum and muscle fibers (G,H). At rupture sites, basement membrane remains attached to sarcolemma (G,H, arrows) and is torn away with fiber detachment and retraction (F, arrow). Contrary to control (E), fibroblasts (fb) are observed in damaged myosepta (F-H). ms, myosepta; mf, muscle fiber.

myosepta showed substantial ultrastructural defects. Wild-type myosepta consist of tightly packed collagen fiber bundles with an oblique arrangement (Fig. 4C,E). By striking contrast, myosepta of MO22-injected larvae appeared distended with sparse unorganized collagen fibrils, even in the absence of muscle cell detachment (Fig. 4D,F). In agreement with the reduced fibril density observed in morphant myosepta, qRT-PCR analysis of *col1a1a* (encoding the fibril-forming collagen I) expression revealed progressive downregulation as embryos developed (supplementary material Fig. S4B). In addition, unlike controls (Fig. 4C,E), damaged myosepta contained numerous fibroblasts (Fig. 4D,F-H). Triple immunofluorescence staining with antibodies to the myoseptal marker COLXII confirmed that loss of COLXXII affects the structure of myosepta that appeared widened, distorted and irregular, and contained numerous Hoechst-positive elongated cells (compare Fig. 5B with control in 5A). Finally, F-actin staining revealed that instead of being regularly packed (Fig. 5A), muscle fibers of morphants appeared twisted and slack (Fig. 5B). Our data imply that damaged myosepta and MTJ may not be stiff enough to function optimally, resulting in a reduced tensile strength and defective muscle fiber packing.

Numerous tears (Fig. 4G,H) were observed in the vertical myosepta of MO22-injected larvae. The BM remained firmly attached to sarcolemma but interactions with the myoseptal collagen fibrils were disrupted (Fig. 4G,H). Accordingly, when muscle fiber has detached (Fig. 4F), an interruption of the BM was observed at the rupture site, indicating that the BM has retracted with the muscle fibers (Fig. 4F). We next performed confocal double immunostaining with antibodies to the BM component laminin and to the sarcomeric α-actinin to examine whether laminin epitopes retract with detached fiber ends (Fig. 5C,D). Laminin antibodies primarily stained the MTJ of uninjected (Fig. 5C) and MO22-injected (Fig. 5D) larvae but the MTJ in MO22-injected larvae appeared distorted and irregular (Fig. 5D). In accordance with TEM observations, we observed that laminin epitopes retracted with detached fiber ends (Fig. 5D), indicating that BM component laminin remained associated with sarcolemma when muscle fibers detach and retract. In all, these results indicate that loss of COLXXII alters the interactions between muscle BM and myoseptal collagen fibrils at MTJ, predisposing to muscle cell detachment.

COLXXII functionally and structurally interacts with integrin α7β1 linkage system

The attachment of muscle fibers to ECM is mainly mediated by the integrin α7 and dystrophin-glycoprotein complex (DGC). In skeletal muscle, the BM component laminin α2 interacts with DGC α-dystroglycan and integrin α7β1, and thereby connects sarcolemma to ECM. Given similarities of their localization at the MTJ and phenotypes (impaired motility behavior, defective MTJ, reduced mechanical stability), we hypothesized that COLXXII may interact with transmembrane or extracellular components of the major linkage systems, such as the integrin α7 (*itag7*), laminin α2 (*lama2*) and/or α-dystroglycan (*dag1*). COLXXII belongs to the FACIT subset of the collagen family, the members of which are characterized by their capacity to mediate protein-protein interactions (Ricard-Blum and Ruggiero, 2005). To determine

Development (2013) doi:10.1242/dev.096024

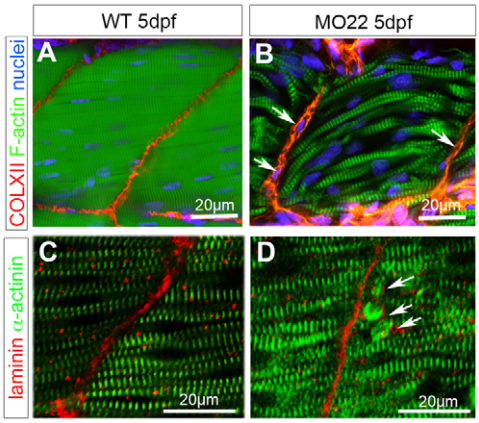

Fig. 5. Whole-mount confocal immunofluorescence. (A,C) Uninjected wild-type (WT) and (B,D) MO22-injected (MO22) larvae at 5 dpf stained with (A,B) anti-COLXII (red), F-actin (green) and Hoescht solution (blue); and (C,D) laminin (red) and α-actinin (green) antibodies. (A,B) MO22-injected myosepta (B) contain numerous Hoechst-positive cells (blue, arrows). (C,D) Arrows in D indicate laminin epitope (red) retraction with detached muscle cells (green) in MO22-injected larvae.

whether COLXXII is a novel player of one or both of the linkage systems, we conducted gene interaction assays as described (Carney et al., 2010) (Fig. 6). For that, we first determined sub-phenotypic doses of morpholinos against each gene and injected MO22 and MO-*itga7*, MO-*lama2* or MO-*dag1* into one-cell embryos at the indicated doses, either alone or in combination, and assessed the occurrence of muscle fiber detachments in injected embryos at 72 hpf (Fig. 6). Only a few embryos (from 0 to 20%) displayed muscle detachment phenotype when morpholinos were injected individually at low doses (Fig. 6A-C). When combined, sub-phenotypic doses of MO22 and MO-*itga7* dramatically increased the percentage of embryos with muscle detachment (Fig. 6A), whereas co-injection of MO22 with MO-*dag1* failed to substantially compromise muscle attachment (Fig. 6C). In accordance with previous work demonstrating that laminin α2 interacts both with integrin α7β1 and dystroglycan, synergistic interactions were similarly observed upon injection of MO-*lama2* with either MO-*dag1* or MO-*itga7* (Fig. 6D). Besides, co-injection of MO22 and MO-*lama2* had lower effect (Fig. 6B) than combination of MO22 and MO-*itga7* (Fig. 6A), suggesting that additional laminin isoforms may be involved in muscle attachments. Overall, our data suggest that zebrafish COLXXII primary interacts with the integrin α7 linkage complex.

The dystrophic phenotype is rescued by micro-injection of human COLXXII protein

The next issue we addressed was whether zebrafish and human COLXXII are functionally equivalent. For that, we performed protein rescue of the MO22-injected embryo phenotype with the human recombinant protein COLXXII (hCOLXXII) produced and purified as described (supplementary material Fig. S6). One-cell stage embryos were co-injected with purified hCOLXXII and 0.5 pmol MO22 and compared with uninjected larvae and with larvae injected with hCOLXXII or MO22 alone. A significant rescue of the phenotype was achieved by co-injecting 0.16 ng of the human COLXXII with 0.5 pmol of MO22, as judged by their morphology (Fig. 7A-C, Table 2) and ability to respond to touch-evoked stimulations (supplementary material Movie 3). As controls, different combinations of co-injections were performed. Injections (n=3) of recombinant human collagen V (Bonod-Bidaud et al., 2007) with MO22 or hCOLXXII with 0.5 pmol morpholinos for the cartilaginous collagen XI (Baas et al., 2009) had no impact on the phenotype rescue (4% of unaffected embryos, n=150; 11% of unaffected embryos, n=150, respectively). Challenging the MO22-injected larvae with repeated electric shocks led to a considerable increase of the severity of the muscle phenotype (Fig. 7E), but had almost no effect on myotome integrity of larvae co-injected with MO22 and the human COLXXII protein (Fig. 7F) as for wild type (Fig. 7D). TEM examination of the skeletal muscle of MO22-injected larvae confirmed the above TEM observations: distended myosepta with sparse collagen fibrils, strong reduction of the sarcolemma folds and loose muscle attachments (Fig. 7H). By contrast, skeletal muscle fibers, MTJs and myosepta of MO22/hCOLXXII-co-injected larvae (Fig. 7I) appeared similar to uninjected larvae (Fig. 7G) though subtle differences in myoseptal collagen fibril density and MTJ folds persisted. In all, the rescue experiments provide evidence for a conserved function of COLXXII in humans.

DISCUSSION

In this study, we have cloned and characterized the zebrafish *col22a1* and shown that its protein product COLXXII, expressed primary by skeletal muscle, is a component of developing and mature MTJ. The spatio-temporal expression profile of *col22a1* is compatible with a function in the stabilization of muscle attachments. First, COLXXII protein was detected in myotomes when fast muscle cells have already elongated and attached to vertical myosepta (Blagden et al., 1997; Henry et al., 2005; Snow and Henry, 2009; Charvet et al., 2011). Second, as embryos developed, *col22a1* transcript strictly localized at trunk and tail muscle fiber ends where they attach to myosepta and the protein was deposited at the MTJ. Expression of COLXXII in mouse embryos has not been reported yet. However, *col22a1* mRNA expression and protein distribution in perinatal and adult mice are consistent with our data (Koch et al., 2004). Third, levels of transcript and protein rose considerably when skeletal muscle contractions increased within chorions and then at hatching, suggesting that expression is regulated by mechanical stress as reported for the sarcomeric protein Tcap (Zhang et al., 2009). In support of this assumption, treatment of embryos with anesthetic reduced COLXXII levels significantly.

Knockdown of COLXXII resulted in a gross phenotype similar to that previously reported for the ‘dystrophic’ class of mutants *sapje* (*sap*, dystrophin), *candyfloss* (*caf*, laminin α2), *lost-contact* (*loc*) also called *ilk* (integrin-linked kinase), *patchytail* also called *dag1* (dystroglycan) (Bassett et al., 2003; Hall et al., 2007; Postel et al., 2008; Gupta et al., 2011), and *itga7* (integrin α7) morphants (Postel et al., 2008), all components of the muscle linkage systems present at the MTJ. Although *col22a1* morphants display a dystrophic phenotype, muscle lesions observed in *col22a1* morphants were considerably less severe than in the *caf*/*lama2* and *loc/ilk* mutants for which massive muscle detachment was observed in individual somites (Hall et al., 2007; Postel et al., 2008). Muscle fiber detachment occurred spontaneously in some *col22a1* morphants but was greatly enhanced when morphants were challenged with high-frequency electrically elicited contractures or with repeated touch-evoked stimuli. Nevertheless, COLXXII knockdown led to a highly significant reduction of muscle force. Because of the apparent integrity of the muscle fiber contractile apparatus, as judged by TEM, confocal microscopy and expression of the late muscle differentiation MHC marker, muscle weakness of *col22a1*

Development (2013) doi:10.1242/dev.096024

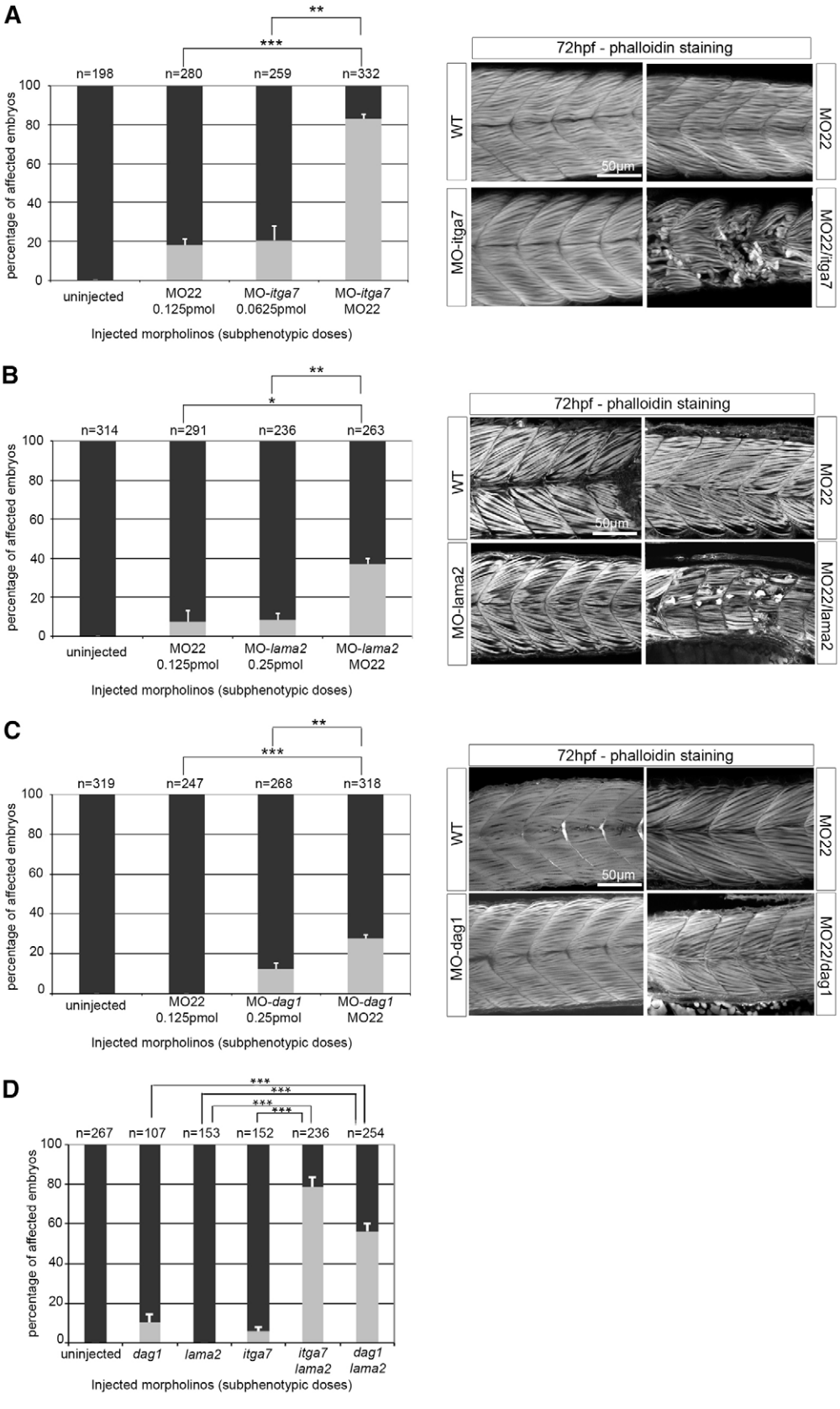

Fig. 6. Genetic interaction between *col22a1* and *itga7*. Synergistic genetic interactions between zebrafish *col22a1* (COLXXII) and *itga7* (integrin α7β1) (A), *lama2* (laminin α2) (B) or *dag1* (dystroglycan) (C), and between *lama2* and *itga7* or *dag1* (D), and mean frequencies of muscle detachment phenotype observed in morphants. Images show lateral views of 72 hpf embryo tail musculature stained with phalloidin-rhodamine after injection, alone or in combination, of sub-phenotypic doses of morpholinos against *col22a1*, *itga7* (A), *lama2* (B) and *dag1* (C). Scale bars: 50 µm. Data are mean±s.e.m. (*n*=3). ***P<0.001; **P<0.01.

morphants was instead attributable to a reduction of force transmission capacity together with fiber detachment that contributed to reduced number of contracting fibers. In accordance with this line of reasoning, myosepta of *col22a1* morphants exhibited loosely packed and low-density collagen fibrils compared with the densely packed collagen fibrils of wild-type myosepta, likely causing tissues to respond inefficiently to contractile force and vulnerability to mechanical stress. TEM examination of the

Development (2013) doi:10.1242/dev.096024

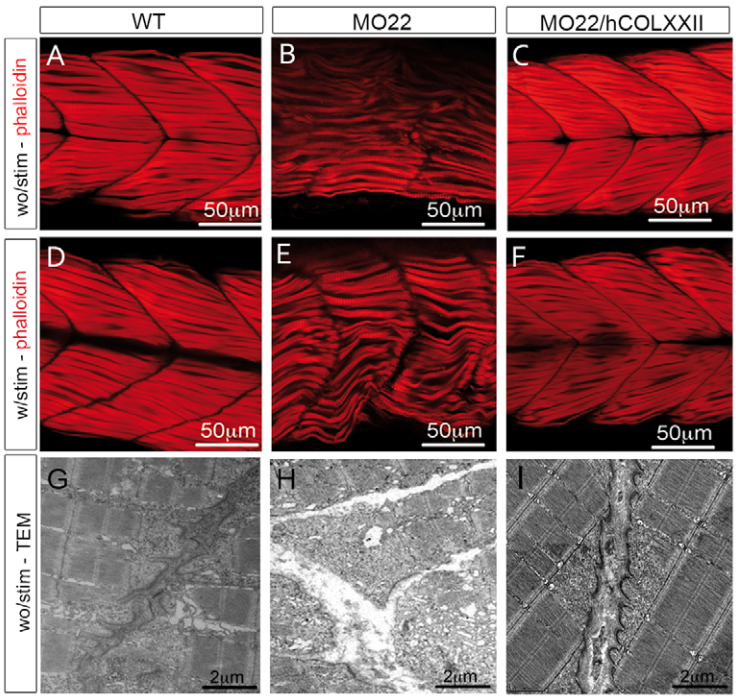

Fig. 7. Protein rescue of MO22-injected embryos. (A-F) 72 hpf and (G-I) 5 dpf uninjected (WT) and embryos injected with 0.16 ng hCOLXXII protein, with 0.5 pmol MO22 or in combination (MO22+hCOLXXII). (A-F) Whole-mount fluorescence staining with phalloidin-rhodamine of embryos stimulated (w/stim, D-F) or not (wo/stim, A-C) with high-frequency field. (G-I) TEM micrographs of skeletal muscle at 5 dpf. Scale bars: 50 µm in A-F; 2 µm in G-I.

dystrophic mutants *patchytail*/*dag1* (Gupta et al., 2011) and *soft*/*lamb2* mutants (Jacoby et al., 2009) also revealed noticeable defects in myoseptal structure. In addition to myoseptal defects, a strong reduction of sarcolemma folds at the MTJ was observed in *col22a1* morphants, as reported in mice models for muscular dystrophy, such as in *itga7*-null mice (Miosge et al., 1999), *mdx* mice (Law and Tidball, 1993; Law et al., 1995) and the double mutants *mdx*/*itga7*$^{-/-}$ and *itga7*/*utr*$^{-/-}$ (utrophin) (Rooney et al., 2006; Welser et al., 2009), but not reported in any of the zebrafish dystrophic class mutants. Reduction of MTJ folds and lack of myoseptal stiffness may also compromise force transmission and likely contributed to fragile muscle attachments. A unique feature of the *col22a1* morphants was the presence of numerous fibroblasts in damaged myosepta. Fibroblasts that are high producers of fibrillar collagens may have been recruited to repair the damaged myosepta, as reported in the tendon-healing process (Wang, 2006). Taken together, our results show that COLXXII contributes to the stabilization and maintenance of muscle attachments and efficient transmission of contractile forces.

Because the onset of COLXXII expression occurred at 24 hpf when the formation/maturation of BM is not completed (Charvet et al., 2011), one can expect that lack of COLXXII would affect junctional BM formation. However, *col22a1* morphants displayed a continuous BM, though irregular in thickness, suggesting that COLXXII is involved in BM maturation but not required for BM initial assembly. Similarly, no ultrastructural defects were reported in junctional BM in absence of perlecan (Zoeller et al., 2008) or laminin α2 (Hall et al., 2007), though the two proteins are major BM components. With TEM, we demonstrated that muscle detachment occurs at junctional extracellular matrix, between the outer surface of BM and the adjacent myoseptal collagen fibers. This result is consistent with the immunogold localization of COLXXII at the outer surface of mouse skeletal muscle BM (Koch et al., 2004).

Interestingly, we showed that muscle detachment is accompanied by induction of Akt signaling pathway. Elevated Akt signaling was found in skeletal muscle in dystrophic mouse models and in individuals with muscular dystrophy (Peter and Crosbie, 2006). Akt treatment of *mdx* mice counteracted muscle wasting by promoting muscle regeneration (Kim et al., 2011). In addition, compensatory increased α7β1 integrin levels in dystrophin-deficient mice were found to confer a protective effect in dystrophic muscle through the activation of ILK/Akt signaling pathway (Boppart et al., 2011). Elevated Akt activation in *col22a1* morphants can thus represent a compensatory response to counteract muscle injury in zebrafish.

In line with the aforementioned role of COLXXII in the stabilization of muscle attachments and given the phenotype similarities to dystrophic mutants, we assessed the *in vivo* contribution of COLXXII in DGC and/or integrin linkage systems by conducting *in vivo* synergistic interactions. The synergistic interactions data point to a role of COLXXII in stabilizing muscle

Table 2. Muscle phenotypes in treated embryos

			Phenotype (%)		
Injection	Number of injections	Number of embryos	Wild type	Muscle detachment	Other
None	3	250	99	0	1
MO22	3	350	4	90	6
hCOLXXII	3	250	86	0	14
MO22 + hCOLXXII	3	500	86	9	5

Percentage of uninjected embryos and embryos injected embryos with 0.5 pmol MO22 or 0.16 µg hCOLXXII alone or in combination (MO22+hCOLXXII) that display muscle phenotype (without stimulation) as scored visually under a stereoscope.

Development (2013) doi:10.1242/dev.096024

attachment through the integrin α7β1 linkage system. This is not surprising because, as a FACIT collagen (Ricard-Blum and Ruggiero, 2005; Veit et al., 2006; Agarwal et al., 2012), COLXXII is well suited to engage molecular interactions and to incorporate protein complexes. Recently, we showed that the FACIT collagen XIV participates to epidermal-dermal cohesion in developing zebrafish (Bader et al., 2013). However, whether COLXXII binding to integrin is direct or indirect is questionable. Although we cannot exclude a direct interaction with integrin, because recombinant human COLXXII was reported to interact with α2β1 integrin-expressing cells (Koch et al., 2004), the fact that disruption occurred external to BM without compromising sarcolemmal integrity supports an indirect interaction. However, co-injection of sub-phenotypic doses of *col22a1* and *lama2* morpholinos elicited weaker phenotype than that generated with co-injection of *col22a1* and *itga7* morpholinos. In addition, although *lama2* was shown to participate in both DGC and integrin linkage systems, double injection of *dag1* and *col22a1* morpholinos at subphenotypic doses revealed that COLXXII does not primary participate to the DGC. These results suggest that, in addition to laminin α2, COLXXII may interact with α7β1 through binding to another laminin isoform. Indeed, developing myotomes express several isoforms (Sztal et al., 2011) and epistasis experiments in zebrafish suggest that different laminin isoforms contribute to muscle attachments and integrity (Sztal et al., 2012). Knockdown of *lama4* or *itga7* resulted in a loss of ILK at the MTJs, which provides evidence that laminin α4 is also involved in muscle attachments (Postel et al., 2008). Collectively, our results suggest that COLXXII is a constitutive protein of the transmembrane α7β1 linkage system that connects BM to the myoseptal extracellular matrix at the MTJ.

The specialized ECM that surrounds muscle cells as they differentiate is thought to play an important role in the formation, maintenance and integrity of muscle. Supporting this assumption, the number of causative extracellular matrix genes associated with muscular dystrophies is expanding (Lisi and Cohn, 2007). Zebrafish represent an excellent model for this group of disorders as *sap*, *caf* and *patchytail* mutants, and morphants in *itg7a*, display compromised muscle attachments that result in muscular dystrophies of various severities (Ingham, 2009) and also for understanding collagen function (Pagnon-Minot et al., 2008; Baas et al., 2009; Bader et al., 2013). The dystrophic phenotype of the *col22a1* morphants and its rescue with injection of the human recombinant protein together with the high sequence conservation between the zebrafish *col22a1* gene and their vertebrate homologs, strongly support a conserved role of COLXXII in humans and qualifies *COL22A1* as a candidate gene for muscular dystrophies in humans. Further research should therefore concentrate on the investigation of mutations in *COL22A1* gene in defined groups of individuals with unresolved cases of muscular dystrophies.

MATERIALS AND METHODS

Zebrafish strain, maintenance and specific treatments

AB/TU wild-type maintenance, embryo collection and staging were carried out at the zebrafish facilities using established protocols (Bader et al., 2009) (PRECI, SFR Lyon Biosciences Gerland). The developmental stages are given in hours post-fertilization (hpf) and days post-fertilization (dpf) at 28.5°C, according to morphological criteria. From 24 hpf, embryos were treated with phenylthiourea (Sigma P7629) to prevent pigmentation. To prevent muscle contraction, embryos were treated with tricaine as described previously (Renaud et al., 2011). Embryos were raised in Danieau solution containing 0.008% tricaine from 10 hpf onwards and replaced every 24 hours.

col22a1 cloning and RT-PCR

Zebrafish total RNA was isolated from 24 hpf embryos using TRIZOL reagent (Invitrogen) and reverse transcribed with SuperScript II Reverse Transcriptase (Life Technologies) and oligo(dT)$_{15}$. Full-length zebrafish *col22a1* was PCR amplified with Phusion High-Fidelity DNA Polymerase (New England BioLabs) using specific primers (supplementary material Table S1). The PCR product was gel purified and cloned into pCR-Blunt II-TOPO (Invitrogen). The sequence obtained was submitted to the EMBL Sequence Nucleotide Database and registered under the accession number HE_981211.

For standard RT-PCR, total RNA was reverse transcribed with M-MLV reverse transcriptase and random primers (Promega). PCR reactions were performed with taq polymerase (New England Biolabs) and *col22a1 VWA*, *col22a1 COL4*, *col22a1 NC3* and *β-actin* primers (supplementary material Table S1).

qRT-PCR

First-strand cDNA was prepared as described above and amplified by PCR using FastStart Universal SYBR Green Master (ROX) mix (Roche) and specific primers (supplementary material Table S1) using a C1000 Thermal cycler with a CFX96 Real-Time system (Biorad). *beta-actin*, *polr2d*, *tbp* were selected as housekeeping genes using BESTKEEPER (Pfaffl et al., 2004) and used for normalization. Relative transcript abundances were determined as described previously (Pfaffl, 2001). Student's *t*-tests were used to determine statistical significance (n=4).

Whole-mount *in situ* hybridization

Whole-mount *in situ* hybridization was performed as described previously (Bader et al., 2009). Probes were amplified from 24 hpf zebrafish cDNA using *col22a1* VWA and *col22a1* TSPN primers (supplementary material Table S1). Stained embryos were observed with a stereomicroscope or a macroscope (all from Leica) equipped with a digital camera.

Morpholino knockdown

Two morpholinos targeting non-overlapping sequences upstream to the *col22a1* start codon (MO22a 5′-CATGAAGTTGCTGCTCCTGTGGAGA-3′, MO22b 5′-CCTGAGCCCAAATCGAAACTCCATC-3′), and a control mismatch morpholino (MS22 5′-CCT**C**AG**G**CCAAAT**G**GAAA-**A**TC**A**ATC-3′) were purchased from Gene Tools (OR, USA) and 0.5 pmol were injected into one- to two-cell embryos as described previously (Pagnon-Minot et al., 2008). Unfertilized eggs were removed at 3 hpf and 50 to 200 embryos were then kept for gross phenotype analysis and remaining eggs were processed as described below.

For gene interaction assays, the integrin α7-ATG morpholinos (MO-*itga7*) (Postel et al., 2008), laminin-α2-MO (MO-*lama2*) (Pollard et al., 2006), dystroglycan-MO (MO-*dag1*) (Parsons et al., 2002) were used. Sub-phenotypic doses determined for each morpholino (0.0625 pmol for MO-*itga7*, 0.125 pmol for MO22a, 0.25 pmol for MO-*dag1* and MO-*lama2*) were used for co-injection into one-cell stage embryos. Morphological and phenotypic observations of morphants were performed with a stereomicroscope or a light microscope (all from Leica) equipped with a digital camera. Muscle detachment was scored when at least one somite was affected.

Immunostaining and antibodies

Whole-mount staining was performed as described (Bader et al., 2009). Stained embryos were observed with a Zeiss LSM510 or a Leica SP5 spectral confocal microscope. Images were processed using Adobe Photoshop and ImageJ softwares. For adult fish, frozen samples were embedded in OCT and immunostaining was performed on cryosections.

Rabbit polyclonal antibodies to zebrafish COLXXII were generated as follows. The N-terminal sequence of collagen XXII was amplified using zebrafish cDNA using degenerated primers (forward, 5′-GAYCTGGYCTTYMTCCTGGACAC-3′; reverse, 5′-ACRTGGAAGA-CRTGNGCNSWCTT-3′). The sequence was 100% identical to NW_003336732.1. For the generation of the recombinant VWA zebrafish domain, the coding sequence was amplified (forward, 5′-

CACGCTAGCCAAAGAGCAGGTTGTAAGAACGTCC-3′; reverse, 5′-GTGGGATCCTTACCTGATCTTGTCGATGGCGTCAAAG-3′ primers) and cloned into our PCEP (Invitrogen) modified expression vector. Underlined nucleotides are, respectively, the *Nhe*I and *Bam*HI cloning sites. The production of polyclonal antibodies was performed as described previously (Bader et al., 2009). The following primary and secondary antibodies were also used: antibodies to zebrafish collagen XII α1 (COLXII) (1:200) (Bader et al., 2009); anti-dystrophin (MANDRA-1) from Developmental Studies Hybridoma Bank (University of Iowa, USA) (1:150), anti-α-actinin (A7811) and rabbit anti-laminin (L9393) from Sigma (1:800 and 1:400, respectively); anti-guinea pig IgG Ab coupled to Cy2 and to Cy3 (1:200); anti-rabbit and anti-mouse IgG coupled to Alexa488 (1:500); anti-rabbit IgG coupled to Alexa546 (all from Invitrogen) (1:500). Nuclei were stained with Hoechst solution and F-actin with fluorescent phalloidin conjugates (Sigma).

Birefringence assay

One-cell embryos were injected with 0.25 pmol MO-*itga7*, 0.5 pmol MO-*lama2* or 0.5 pmol MO22. Uninjected and morpholino-injected 4 dpf zebrafish larvae were anesthetized with tricaine, mounted in 1% low melting agarose on a glass slide, placed between two polarizers (3Dlens, Taiwan) and observed with a Leica macroscope equipped with a coolSNAP CCD camera. The mean gray value of pixels in the trunk region was measured with ImageJ software. Values are expressed as the percentage of uninjected larvae±s.e.m. (n=10). Data were analyzed by one-way analysis of variance (ANOVA) followed by Bonferroni's multiple comparison test (GraphPad Prism Software).

Histology and TEM

Zebrafish larvae were processed as previously described (Charvet et al., 2011). Thin sections stained with Methyl-Azur blue were observed with a light microscope (Leica) equipped with a digital camera (Nikon). Ultrathin sections were observed with a Phillips CM 120 electron microscope equipped with a Gatan digital CCD camera at the Centre Technique des Microstructures (UCBL, Villeurbanne, France).

Muscle contraction measurements

Procedure was adapted from Dou et al. (Dou et al., 2008). Zebrafish larvae were anesthetized with 0.017% tricaine and the head was crushed. Larvae were then bathed in a solution containing (in mM) 140 NaCl, 5 KCl, 2.5 $CaCl_2$, 1 $MgCl_2$, 10 HEPES (pH 7.2). The tail was stuck to the bottom of the dish using a small pin while the head was hung on the extended arm of an AE801 force transducer mounted on a micromanipulator that allowed length adjustment. The whole fish musculature was stimulated by applying electric field pulses of 0.5 ms duration using two electrodes placed on either side of the fish. In each larva tested, the voltage was progressively augmented to give maximal twitch response and the voltage selected for investigating maximal force was then further increased by 20%. The larvae were gradually stretched from a resting length up to an optimal length, giving maximal force signal in response to stimulation. The contraction amplitude was measured at the peak of the force signal.

Protein extraction and western blot analyses

Embryos (30/stage/experiment) were sacrificed and yolks and head were discarded. Specimens were then frozen in liquid nitrogen and stored at −80°C until use. Embryos were lysed in 50 mM Tris (pH 8), 150 mM NaCl, 0.5% sodium deoxycholate, 1% Triton X-100, 1% SDS, 10 mM sodium fluoride and 1 mM sodium orthovanadate containing a protease inhibitor cocktail (Complete EDTA-free, Roche). Total extracts were sonicated and 10 µg of proteins were separated by SDS-PAGE and transferred to PVDF membrane. Immunological detection was performed with HRP-conjugated secondary antibodies using Immun-Star WesternC as a substrate (Bio-Rad). The primary antibodies were: rabbit monoclonal anti-phospho-Ser473 Akt (193H12) (1:1000), rabbit polyclonal anti-Akt (1:2000), rabbit monoclonal anti-phospho-Thr202/Tyr204 Erk1/2 (197G2) (1:1000), rabbit monoclonal anti-Erk1/2 (137F5) (1:2000) and rabbit monoclonal anti-GAPDH (14C10) (1:10,000) (Cell Signaling Technology); mouse monoclonal anti-myosin heavy chain antibody (F59, DSHB) (1:100); and mouse monoclonal anti-acetylated tubulin antibody (6-11B-1, Sigma) (1:10,000). Band intensities were quantified using ImageJ software and Student's t-test was used to determine statistical significance.

Touch-evoked escape behavior assay

Live 5 dpf fishes were placed in Danieau buffer. The motility of larvae after stimulation by tail touch was recorded using a macroscope (Macro-Fluo, Leica) with a digital camera system.

Protein rescue

Protein rescue was performed as previously described (Zoeller et al., 2008). Purified recombinant human full-length COLXXII was prepared as previously described (Koch et al., 2004). Recombinant proteins, human COLXXII or human collagen V domain as control (Bonod-Bidaud et al., 2007), were injected in embryos either alone or in combination with morpholino (0.5 pmol) MO22 or *col11a1* morpholinos as control (Baas et al., 2009) as described above. Fifty to 200 embryos were kept for gross phenotype analysis; 5 and 10 larvae were processed for TEM and phalloidin-rhodamine staining respectively.

Acknowledgements

We thank Laure Bernard (PRECI) for fish maintenance and Christophe Chamot (PLATIM) for expert image analysis (SFR Lyon-Biosciences-Gerland), the 'Centre Technique des Microstructures' (UCBL, Villeurbanne) for technical assistance with transmission electron microscopy and Pauline Nauroy for sharing qRT-PCR primers.

Competing interests

The authors declare no competing financial interests.

Author contributions

B.C. performed and analyzed all experiments reported in Fig. 1A,B,D, Fig. 2B-D, Fig. 3A,B, Fig. 5 and Fig. 7; A.G. performed and analyzed all experiments reported in Table 1, Fig. 1C, Fig. 2A, Fig. 3C and all experiments reported in supplementary material Fig. S1, Fig. S2, Fig. S3B and Fig. S5. M.M. performed and analyzed experiments reported in Figs 4 and 6 and contributed to some experiments in Figs 5 and 7 and supplementary material. D.Z. and J.S. produced and characterized antibodies against zebrafish collagen XXII and the recombinant proteins and contributed to experiments reported in supplementary material Figs S3 and S6. E.G. contributed to some experiments reported in Fig. 6 and subsequent data analysis. S.B. designed, performed and analyzed the experiment reported in Fig 2E. H.L.B. and C.M. contributed to Fig. 1B and Fig. 3C, respectively. B.A. designed, supervised and analyzed all experiments reported in Fig. 3A. M.K. designed and supervised production of antibodies and recombinant proteins and subsequent data analysis. B.C., A.G., B.A. and M.K. helped with manuscript editing and critical review. F.R. supervised all experimental design, analyzed all data and wrote the manuscript.

Funding

This work was supported by the Agence Nationale de la Recherche [10BLAN121901], by the Région Rhône-Alpes (Cible) and Association Française contre les Myopathies [MNM1-2010] to F.R.; by the Köln Fortune Programm to M.K. and D.Z.; and by the Fondation pour la Recherche Médicale to B.C.

Supplementary material

Supplementary material available online at
http://dev.biologists.org/lookup/suppl/doi:10.1242/dev.096024/-/DC1

References

Agarwal, P., Zwolanek, D., Keene, D. R., Schulz, J. N., Blumbach, K., Heinegård, D., Zaucke, F., Paulsson, M., Krieg, T., Koch, M. et al. (2012). Collagen XII and XIV, new partners of cartilage oligomeric matrix protein in the skin extracellular matrix suprastructure. *J. Biol. Chem.* **287**, 22549-22559.

Baas, D., Malbouyres, M., Haftek-Terreau, Z., Le Guellec, D. and Ruggiero, F. (2009). Craniofacial cartilage morphogenesis requires zebrafish col11a1 activity. *Matrix Biol.* **28**, 490-502.

Bader, H. L., Keene, D. R., Charvet, B., Veit, G., Driever, W., Koch, M. and Ruggiero, F. (2009). Zebrafish collagen XII is present in embryonic connective tissue sheaths (fascia) and basement membranes. *Matrix Biol.* **28**, 32-43.

Bader, H. L., Lambert, E., Guiraud, A., Malbouyres, M., Driever, W., Koch, M. and Ruggiero, F. (2013). Zebrafish collagen XIV is transiently expressed in epithelia and is required for proper function of certain basement membranes. *J. Biol. Chem.* **288**, 6777-6787.

Bassett, D. I., Bryson-Richardson, R. J., Daggett, D. F., Gautier, P., Keenan, D. G. and Currie, P. D. (2003). Dystrophin is required for the formation of stable muscle attachments in the zebrafish embryo. *Development* **130**, 5851-5860.
Blagden, C. S., Currie, P. D., Ingham, P. W. and Hughes, S. M. (1997). Notochord induction of zebrafish slow muscle mediated by Sonic hedgehog. *Genes Dev.* **11**, 2163-2175.
Bonod-Bidaud, C., Beraud, M., Vaganay, E., Delacoux, F., Font, B., Hulmes, D. J. and Ruggiero, F. (2007). Enzymatic cleavage specificity of the proalpha1(V) chain processing analysed by site-directed mutagenesis. *Biochem. J.* **405**, 299-306.
Boppart, M. D., Burkin, D. J. and Kaufman, S. J. (2011). Activation of AKT signaling promotes cell growth and survival in α7β1 integrin-mediated alleviation of muscular dystrophy. *Biochim. Biophys. Acta* **1812**, 439-446.
Carmignac, V. and Durbeej, M. (2012). Cell-matrix interactions in muscle disease. *J. Pathol.* **226**, 200-218.
Carney, T. J., Feitosa, N. M., Sonntag, C., Slanchev, K., Kluger, J., Kiyozumi, D., Gebauer, J. M., Coffin Talbot, J., Kimmel, C. B., Sekiguchi, K. et al. (2010). Genetic analysis of fin development in zebrafish identifies furin and hemicentin1 as potential novel fraser syndrome disease genes. *PLoS Genet.* **6**, e1000907.
Charvet, B., Malbouyres, M., Pagnon-Minot, A., Ruggiero, F. and Le Guellec, D. (2011). Development of the zebrafish myoseptum with emphasis on the myotendinous junction. *Cell Tissue Res.* **346**, 439-449.
Cohn, R. D. and Campbell, K. P. (2000). Molecular basis of muscular dystrophies. *Muscle Nerve* **23**, 1456-1471.
Desaki, J. (1992). Scanning electron microscopical study of skeletal muscle fiber ends in normal and dystrophic mice. *Arch. Histol. Cytol.* **55**, 449-452.
Dou, Y., Andersson-Lendahl, M. and Arner, A. (2008). Structure and function of skeletal muscle in zebrafish early larvae. *J. Gen. Physiol.* **131**, 445-453.
Gupta, V., Kawahara, G., Gundry, S. R., Chen, A. T., Lencer, W. I., Zhou, Y., Zon, L. I., Kunkel, L. M. and Beggs, A. H. (2011). The zebrafish dag1 mutant: a novel genetic model for dystroglycanopathies. *Hum. Mol. Genet.* **20**, 1712-1725.
Guyon, J. R., Goswami, J., Jun, S. J., Thorne, M., Howell, M., Pusack, T., Kawahara, G., Steffen, L. S., Galdzicki, M. and Kunkel, L. M. (2009). Genetic isolation and characterization of a splicing mutant of zebrafish dystrophin. *Hum. Mol. Genet.* **18**, 202-211.
Hall, T. E., Bryson-Richardson, R. J., Berger, S., Jacoby, A. S., Cole, N. J., Hollway, G. E., Berger, J. and Currie, P. D. (2007). The zebrafish candyfloss mutant implicates extracellular matrix adhesion failure in laminin alpha2-deficient congenital muscular dystrophy. *Proc. Natl. Acad. Sci. USA* **104**, 7092-7097.
Han, R., Kanagawa, M., Yoshida-Moriguchi, T., Rader, E. P., Ng, R. A., Michele, D. E., Muirhead, D. E., Kunz, S., Moore, S. A., Iannaccone, S. T. et al. (2009). Basal lamina strengthens cell membrane integrity via the laminin G domain-binding motif of alpha-dystroglycan. *Proc. Natl. Acad. Sci. USA* **106**, 12573-12579.
Hayashi, Y. K., Chou, F. L., Engvall, E., Ogawa, M., Matsuda, C., Hirabayashi, S., Yokochi, K., Ziober, B. L., Kramer, R. H., Kaufman, S. J. et al. (1998). Mutations in the integrin alpha7 gene cause congenital myopathy. *Nat. Genet.* **19**, 94-97.
Helbling-Leclerc, A., Zhang, X., Topaloglu, H., Cruaud, C., Tesson, F., Weissenbach, J., Tomé, F. M., Schwartz, K., Fardeau, M., Tryggvason, K. et al. (1995). Mutations in the laminin alpha 2-chain gene (LAMA2) cause merosin-deficient congenital muscular dystrophy. *Nat. Genet.* **11**, 216-218.
Henry, C. A., McNulty, I. M., Durst, W. A., Munchel, S. E. and Amacher, S. L. (2005). Interactions between muscle fibers and segment boundaries in zebrafish. *Dev. Biol.* **287**, 346-360.
Ingham, P. W. (2009). The power of the zebrafish for disease analysis. *Hum. Mol. Genet.* **18** R1, R107-R112.
Jacoby, A. S., Busch-Nentwich, E., Bryson-Richardson, R. J., Hall, T. E., Berger, J., Berger, S., Sonntag, C., Sachs, C., Geisler, R., Stemple, D. L. et al. (2009). The zebrafish dystrophic mutant softy maintains muscle fibre viability despite basement membrane rupture and muscle detachment. *Development* **136**, 3367-3376.
Kawahara, G., Karpf, J. A., Myers, J. A., Alexander, M. S., Guyon, J. R. and Kunkel, L. M. (2011). Drug screening in a zebrafish model of Duchenne muscular dystrophy. *Proc. Natl. Acad. Sci. USA* **108**, 5331-5336.
Kim, M. H., Kay, D. I., Rudra, R. T., Chen, B. M., Hsu, N., Izumiya, Y., Martinez, L., Spencer, M. J., Walsh, K., Grinnell, A. D. et al. (2011). Myogenic Akt signaling attenuates muscular degeneration, promotes myofiber regeneration and improves muscle function in dystrophin-deficient mdx mice. *Hum. Mol. Genet.* **20**, 1324-1338.
Koch, M., Schulze, J., Hansen, U., Ashwodt, T., Keene, D. R., Brunken, W. J., Burgeson, R. E., Bruckner, P. and Bruckner-Tuderman, L. (2004). A novel marker of tissue junctions, collagen XXII. *J. Biol. Chem.* **279**, 22514-22521.
Law, D. J. and Tidball, J. G. (1993). Dystrophin deficiency is associated with myotendinous junction defects in prenecrotic and fully regenerated skeletal muscle. *Am. J. Pathol.* **142**, 1513-1523.
Law, D. J., Caputo, A. and Tidball, J. G. (1995). Site and mechanics of failure in normal and dystrophin-deficient skeletal muscle. *Muscle Nerve* **18**, 216-223.
Lisi, M. T. and Cohn, R. D. (2007). Congenital muscular dystrophies: new aspects of an expanding group of disorders. *Biochim. Biophys. Acta* **1772**, 159-172.
Miosge, N., Klenczar, C., Herken, R., Willem, M. and Mayer, U. (1999). Organization of the myotendinous junction is dependent on the presence of alpha7beta1 integrin. *Lab. Invest.* **79**, 1591-1599.
Mohamed, J. S., Lopez, M. A., Cox, G. A. and Boriek, A. M. (2010). Anisotropic regulation of Ankrd2 gene expression in skeletal muscle by mechanical stretch. *FASEB J.* **24**, 3330-3340.
Ng, M. C., Hsu, C. P., Wu, Y. J., Wu, S. Y., Yang, Y. L. and Lu, K. T. (2012). Effect of MK-801-induced impairment of inhibitory avoidance learning in zebrafish via inactivation of extracellular signal-regulated kinase (ERK) in telencephalon. *Fish Physiol. Biochem.* **38**, 1099-1106.
Pagnon-Minot, A., Malbouyres, M., Haftek-Terreau, Z., Kim, H. R., Sasaki, T., Thisse, C., Thisse, B., Ingham, P. W., Ruggiero, F. and Le Guellec, D. (2008). Collagen XV, a novel factor in zebrafish notochord differentiation and muscle development. *Dev. Biol.* **316**, 21-35.
Parsons, M. J., Campos, I., Hirst, E. M. and Stemple, D. L. (2002). Removal of dystroglycan causes severe muscular dystrophy in zebrafish embryos. *Development* **129**, 3505-3512.
Peter, A. K. and Crosbie, R. H. (2006). Hypertrophic response of Duchenne and limb-girdle muscular dystrophies is associated with activation of Akt pathway. *Exp. Cell Res.* **312**, 2580-2591.
Pfaffl, M. W. (2001). A new mathematical model for relative quantification in real-time RT-PCR. *Nucleic Acids Res.* **29**, e45.
Pfaffl, M. W., Tichopad, A., Prgomet, C. and Neuvians, T. P. (2004). Determination of stable housekeeping genes, differentially regulated target genes and sample integrity: BestKeeper—Excel-based tool using pair-wise correlations. *Biotechnol. Lett.* **26**, 509-515.
Pollard, S. M., Parsons, M. J., Kamei, M., Kettleborough, R. N., Thomas, K. A., Pham, V. N., Bae, M. K., Scott, A., Weinstein, B. M. and Stemple, D. L. (2006). Essential and overlapping roles for laminin alpha chains in notochord and blood vessel formation. *Dev. Biol.* **289**, 64-76.
Postel, R., Vakeel, P., Topczewski, J., Knöll, R. and Bakkers, J. (2008). Zebrafish integrin-linked kinase is required in skeletal muscles for strengthening the integrin-ECM adhesion complex. *Dev. Biol.* **318**, 92-101.
Renaud, O., Herbomel, P. and Kissa, K. (2011). Studying cell behavior in whole zebrafish embryos by confocal live imaging: application to hematopoietic stem cells. *Nat. Protoc.* **6**, 1897-1904.
Ricard-Blum, S. and Ruggiero, F. (2005). The collagen superfamily: from the extracellular matrix to the cell membrane. *Pathol. Biol. (Paris)* **53**, 430-442.
Rooney, J. E., Welser, J. V., Dechert, M. A., Flintoff-Dye, N. L., Kaufman, S. J. and Burkin, D. J. (2006). Severe muscular dystrophy in mice that lack dystrophin and alpha7 integrin. *J. Cell Sci.* **119**, 2185-2195.
Snow, C. J. and Henry, C. A. (2009). Dynamic formation of microenvironments at the myotendinous junction correlates with muscle fiber morphogenesis in zebrafish. *Gene Expr. Patterns* **9**, 37-42.
Sztal, T., Berger, S., Currie, P. D. and Hall, T. E. (2011). Characterization of the laminin gene family and evolution in zebrafish. *Dev. Dyn.* **240**, 422-431.
Sztal, T. E., Sonntag, C., Hall, T. E. and Currie, P. D. (2012). Epistatic dissection of laminin-receptor interactions in dystrophic zebrafish muscle. *Hum. Mol. Genet.* **21**, 4718-4731.
Turner, D. L. and Weintraub, H. (1994). Expression of achaete-scute homolog 3 in Xenopus embryos converts ectodermal cells to a neural fate. *Genes Dev.* **8**, 1434-1447.
Veit, G., Hansen, U., Keene, D. R., Bruckner, P., Chiquet-Ehrismann, R., Chiquet, M. and Koch, M. (2006). Collagen XII interacts with avian tenascin-X through its NC3 domain. *J. Biol. Chem.* **281**, 27461-27470.
Wang, J. H. (2006). Mechanobiology of tendon. *J. Biomech.* **39**, 1563-1582.
Welser, J. V., Rooney, J. E., Cohen, N. C., Gurpur, P. B., Singer, C. A., Evans, R. A., Haines, B. A. and Burkin, D. J. (2009). Myotendinous junction defects and reduced force transmission in mice that lack alpha7 integrin and utrophin. *Am. J. Pathol.* **175**, 1545-1554.
Zhang, R., Yang, J., Zhu, J. and Xu, X. (2009). Depletion of zebrafish Tcap leads to muscular dystrophy via disrupting sarcomere-membrane interaction, not sarcomere assembly. *Hum. Mol. Genet.* **18**, 4130-4140.
Zoeller, J. J., McQuillan, A., Whitelock, J., Ho, S. Y. and Iozzo, R. V. (2008). A central function for perlecan in skeletal muscle and cardiovascular development. *J. Cell Biol.* **181**, 381-394.